

https://doi.org/10.1070/QEL16398

Calculation and experimental verification of a collimator with a Kerr lens for fibre laser mode locking

Ia.V. Zakharov, A.G. Kuznetsov, E.V. Podivilov, S.A. Babin

Abstract. **We present the calculation and experimental verification of the operation of a collimator coupling a light beam into an optical fibre with an As_2S_3 nonlinear plate. It is shown that a Kerr lens formed in the plate with an increase in the peak pulse power leads to an increase in the output coupling ratio by about 15%, which can be used for the passive mode locking of a fibre laser.**

Keywords: *Kerr lens, fibre laser, ultrashort pulses, mode locking.*

1. Introduction

Generation of few-cycle laser pulses is of great interest both for industry and science. High peak powers of pulsed lasers allow the processing of various materials: cutting, drilling, microprofiling [1], while the quality of the products produced increases significantly in comparison with machining. Ultrashort laser pulses make it possible to record extremely short time intervals, which is necessary, for example, in the study of fast processes and the development of new frequency standards [2].

Recently, due to their simplicity, reliability and mobility, fibre lasers have been increasingly used for the generation of ultrashort pulses (USPs) [2]. The generation of ultrashort pulses in a laser should rely on phase matching of the resonator modes, which can be carried out by active or passive methods. Active mode locking is achieved with an acousto-optic or electro-optic modulator, which modulates the resonator losses in exact synchronism with the resonator round trips. Passive mode locking is based on the use of various saturable absorbers, such as SESAM [3], carbon nanotubes [4], graphene [5] and Kerr nonlinearity, leading to amplitude self-modulation due to the nonlinear polarisation evolution (NPE) effect [6] or Kerr lens [7]. The method of mode locking in a laser using a Kerr lens is based on the self-focusing effect of the light in media with a quadratic dependence of the refractive index on the field strength. The Kerr lens is widely used to mode-lock solid-state lasers, in particular Ti:sapphire lasers, where pulses of a few optical cycles are obtained [7]. Wang et al. [8, 9] numerically modelled a Kerr lens for a fibre-optic laser with one of the possible configurations of laser beam coupling into fibre through a nonlinear plate; however, the possibility of application of a Kerr lens in fibre lasers has not yet been studied.

The purpose of this work is to calculate and test experimentally the possibility of using a nonlinear collimator based on a Kerr lens for fibre laser mode locking.

Ia.V. Zakharov, E.V. Podivilov, S.A. Babin Institute of Automation and Electrometry, Siberian Branch, Russian Academy of Sciences, prosp. Akad. Koptyuga 1, 630090 Novosibirsk, Russia; Novosibirsk State University, ul. Pirogova 2, 630090 Novosibirsk, Russia; e-mail: YZWL92@gmail.com;
A.G. Kuznetsov Institute of Automation and Electrometry, Siberian Branch, Russian Academy of Sciences, prosp. Akad. Koptyuga 1, 630090 Novosibirsk, Russia

Received 7 April 2017; revision received 25 July 2017
Kvantovaya Elektronika **47** (10) 882–886 (2017)
Translated by I.A. Ulitkin

2. Model

For the theoretical analysis, we considered a nonlinear deformation of a Gaussian beam, having in the linear limit a waist in the middle of an As_2S_3 nonlinear plate (Fig. 1), within the first-order perturbation theory of the nonlinear Schrödinger equation. The analysis showed that after passing through the self-focusing medium the beam retains its shape, but the position of the waist of the emerging beam shifts with increasing power forward along the direction of the light propagation due to a nonlinear increase in the optical path. According to the calculations, the magnitude of the shift Δ is determined by the expression (see Appendix):

$$\Delta(P, z_{R,0}) = 2\frac{P}{P_{cr,G}} h \frac{z_{R,0}^2}{h^2/2n + z_{R,0}^2}, \qquad (1)$$

where h is the thickness of the nonlinear plate; n is the linear part of the refractive index; $z_{R,0} = kw_0^2/2$ is the Rayleigh length of the beam in vacuum; w_0 is the waist radius; $k = 2\pi/\lambda$ is the wave number; $P_{cr,G} = \lambda^2/(2nn_2)$ is the critical self-focusing power for a Gaussian beam; and n_2 is the nonlinear part of the refractive index.

This effect can be used to obtain amplitude self-modulation in a fibre laser, which requires a collimator for coupling the laser light into optical fibre with a nonlinear element (see Fig. 1). Note that the configuration of our collimator differs

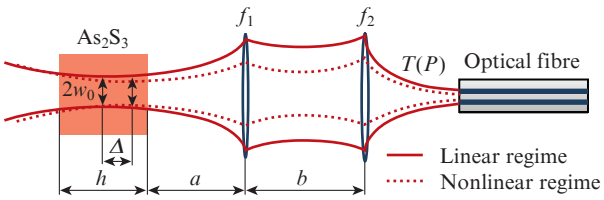

Figure 1. Change in the position of the beam waist Δ in the nonlinear plate (in the linear case, the beam waist w_0 is in the middle of the plate) and the corresponding change in the output coupling ratio of the beam launched into optical fibre $T(P)$ with a collimator consisting of a nonlinear plate and two lenses.

from that calculated in [8, 9]. The output coupling ratio $T(a,b,z_{R,0},x)$ is proportional to the overlap integral of the mode of the optical fibre and incident beam (with the parameter $z_{R,0}$), which in the linear case is determined by the lens parameters (a,b) and the longitudinal detuning x of fibre from the position corresponding to the maximum of the coupling ratio.

With increasing laser power, the position of the beam waist in the plate shifts toward the lens, which is equivalent to changing the distance between the nonlinear plate and the first lens (see Appendix). This leads to the fact that the output coupling ratio T begins to depend on power P and is calculated via the overlap integral $I(a + h/n - \Delta(P,z_{R,0})/n, b, z_{R,0}, x)$ [see formula (A24)].

3. Experiment

To verify the calculations, we assembled an experimental setup shown in Fig. 2.

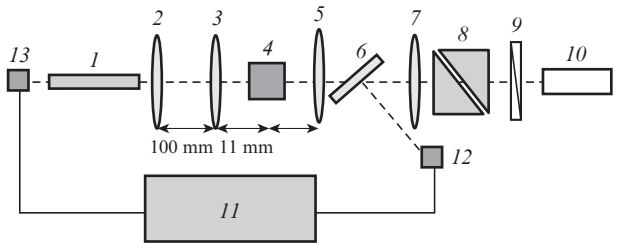

Figure 2. Scheme of the experiment on coupling the laser light into optical fibre using a collimator with a nonlinear element: (*1*) 1060xp optical fibre; (*2*) Thorlabs F240FC-C aspherical lens (f = 8 mm); (*3*) and (*5*) Thorlabs A397TM-C aspherical lenses (f = 11 mm); (*4*) 1.1-mm-thick As_2S_3 plate; (*6*) mirror with a transmission of 10%; (*7*) spherical lens (f = 11 cm); (*8*) Glan prism; (*9*) half-wave plate; (*10*) Nd:YAG laser (λ = 1064 nm, pulse duration τ = 0.6 ns); (*11*) Ophir console with photodetectors (*12*) and (*13*).

In the experiment we used a Standa STA01-07 Nd:YAG laser emitting at a wavelength of 1064 nm with a pulse duration of 0.6 ns and a peak power of up to 140 kW. Lenses (*2*), (*3*) and (*5*) were adjusted in three axes and angles with the help of the corresponding positioners. Elements (*8*) and (*9*) made it possible to control the power of the transmitted beam by rotating a half-wave plate around the beam propagation axis. In this case, the polarisation direction of the light emerging from the half-wave plate rotates, and the Glan prism passes only linear polarisation and couples out the second polarisation component in the perpendicular direction. Lens (*7*) was fixed and neither axis- nor angle-adjustable. Then the beam was incident on filter (*6*), which reflected part of the light and passed part of it ahead. The light reflected at an angle fell on photodetector (*12*). The part of the transmitted beam was focused into the nonlinear plate by lens (*5*). Since this lens is aspherical, it was fixed in a three-axis lens holder on a linear positioner and aligned so that the beam passed through the lens centre. The beam transmitted through the nonlinear plate was collimated by lens (*3*), identical to lens (5). It was also mounted on the alignment positioner. The nonlinear plate could be moved along the beam propagation direction. Then the beam was incident on aspherical lens (*2*) mounted on the positioner to couple the beam into optical fibre (*1*), which could also be moved along the propagation direction of the beam.

The experimental setup was first aligned without the nonlinear element to the maximum of the output coupling ratio. After that, photodetectors (*12*) and (*13*), measuring the power at the input and output of the fibre, were calibrated, and the output coupling ratio was calculated. Next, the nonlinear element was installed (see Fig. 2) and again the setup was aligned to the maximum of the output coupling ratio by adjusting lenses (*3*) and (*5*).

As a nonlinear medium, we used an As_2S_3 plate of thickness h = 1.1 mm with linear and nonlinear refractive indices n_0 = 2.5 and $n_2 = 2.5\times10^{-18}$ m^2 W^{-1}, respectively [10]. In this case, the calculated critical power $P_{cr,G}$ = 27 kW [11]. The maximum nonlinear effect should be expected at $n_0 h = 2z_{R,0}$, when the beam waist is inside the nonlinear glass. For our sample, the maximum effect is achieved at a waist radius of w_0 = 8.5 μm.

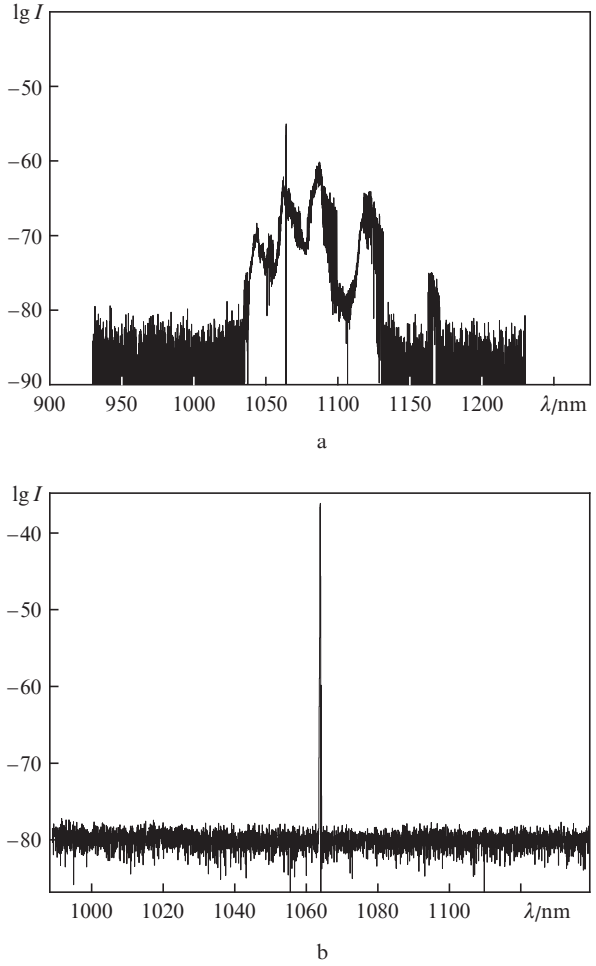

Figure 3. Emission spectrum at the output of (a) a long segment of optical fibre and (b) 10-cm-long optical fibre (after its shortening). The input radiation power is P = 10 kW.

One should also bear in mind that at high laser powers, stimulated Raman scattering occurs in optical fibres. The emission spectrum at the output of a sufficiently long segment of optical fibre, measured with an OSA YOKOGAWA 6370 spectrophotometer is shown in Fig. 3a. In order to get rid of the influence of stimulated Raman scattering, we shortened the length of the fibre to 10 cm. The spectrum of the transmitted light in this case is shown in Fig. 3b.

4. Results

The results of measurements of the output coupling ratio of the beam launched into an optical fibre using a collimator with a nonlinear plate and without it are shown in Fig.4. It can be seen that for the setup without a plate, the losses on bulk optics when the beam is launched into the optical fibre are about 44% and are virtually independent of power. After the plate is inserted, due to Fresnel reflection, approximately 66% passes through the plate, and an increase in the optical path of the beam results in a shift of the maximum of the output coupling ratio by approximately 0.2 mm. As a result, the coupling loss increases, but nevertheless the output coupling ratio increases with increasing power.

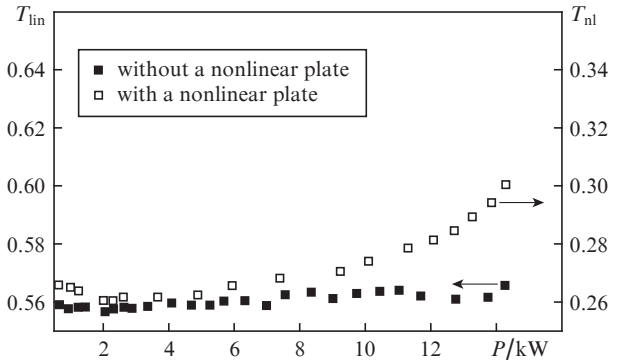

Figure 4. Dependence of the output coupling ratio in optical fibre on the power supplied to the nonlinear plate. The left vertical axis corresponds to $T_{lin}(P)$ without a plate. The right vertical axis corresponds to the dependence of $T_{nl}(P)$ with a plate.

Figure 5a shows the experimental dependence of the output coupling ratio on the power, normalised to the coupling ratio at a low power (at a power close to zero, a large error is introduced by noise). Figure 5b illustrates the calculated dependences of the output coupling ratio on the power, normalised to the coupling ratio at a zero power, for different longitudinal displacements of the end of the optical fibre from the position corresponding to the maximum of the output coupling ratio. As can be seen from Fig. 5b, the calculated $T(P)$ curves increase monotonically at $x = 0.05$ and 0.1 mm and the relative amplitude of the nonlinear modulation reaches 15% at $P/P_{cr,G} \approx 0.5$, which corresponds approximately to the experimentally measured plot (see Fig. 5a) taking into account that $P = 16$ kW is about half of the estimated critical power. Note that the experimental and calculated graphs have different curvatures, which can indicate the presence of an initial detuning of the beam waist from the centre of the plate. In general, for a better comparison of calculations with the experiment, an exact knowledge of the parameters of the experimental setup is required.

5. Conclusions

Thus, the calculation and experiment are in satisfactory agreement with each other. The behaviour of the output coupling ratio with increasing power and its growth by 15% at a power of 16 kW, equal to half of the critical power, qualitatively coincide. The obtained results demonstrate the possibility of creating a passively mode-locked fibre laser using a nonlinear

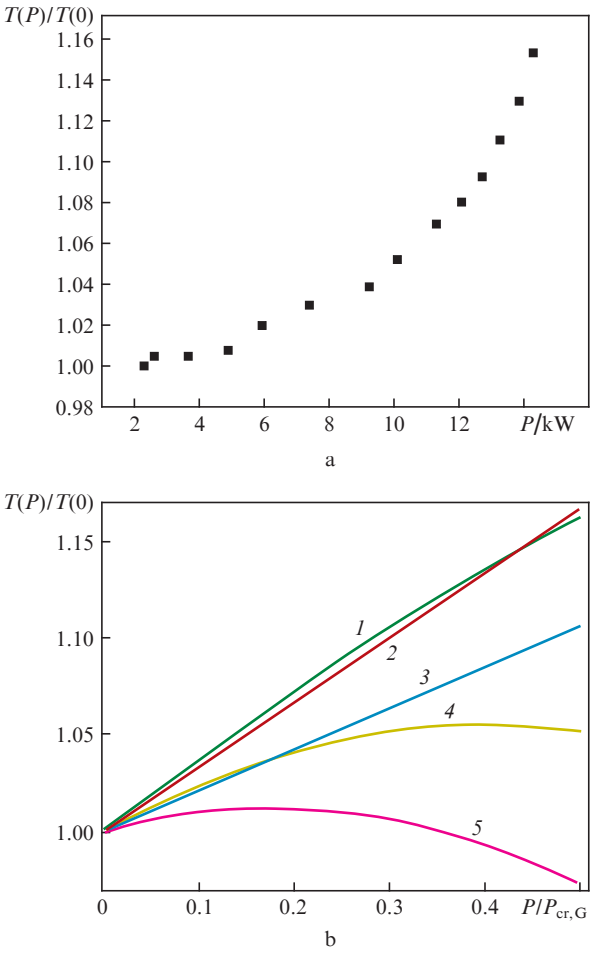

Figure 5. (a) Experimental dependence of the output coupling ratio in optical fibre, normalised to the output coupling ratio at a low power and (b) calculated dependences $T(P)/T(0)$ for different fibre detuning values x = (*1*) 0.05, (*2*) 0.1, (*3*) 0.2, (*4*) 0.3 and (*5*) 0.4 mm.

collimator based on a Kerr lens. We note that this is the simplest version of the application of a Kerr lens in a laser based on a conventional single-mode fibre. Its relative disadvantage is the need to use bulk optics in the resonator. In the literature, the variants of an all-fibre laser with a Kerr lens are theoretically considered (see, e.g., [12]), but in this case it is necessary to have an active waveguide of complex design.

Acknowledgements. The work is supported by the Russian Science Foundation (Project No. 14-22-00118).

Appendix. Calculation of a nonlinear collimator

In a glass with a Kerr nonlinearity, the permittivity ε depends on the electric field amplitude $E = U(r,z)\exp(i\omega t - ikz)$ as [13]

$$\varepsilon = (n + n_2 I)^2 \approx n^2 + 2nn_2|U|^2. \quad \text{(A1)}$$

Then the behaviour of radiation in a nonlinear medium is described by the equation:

$$\Delta_\perp U - 2ink U_z + \frac{4\pi}{P_{cr,G}}|U|^2 U = 0, \quad \text{(A2)}$$

where, according to [11], $P_{cr,G} = \lambda^2/(2\pi n n_2)$ is the critical power at which (in accordance with Talanov's theorem [13]) the self-focusing effect becomes stronger than the diffraction scattering of a Gaussian beam. Let a Gaussian beam have the form

$$U_0 = A\exp\left(-\frac{ik}{2q_0}r^2\right)\exp(-iF_0), \tag{A3}$$

where k is the wave vector in vacuum; F_0 is the real phase; $q = z_0 + iz_{R,0}$; z_0 is the waist position of the beam with the opposite sign; $z_{R,0} = kW_0^2/2$ is the Rayleigh beam length in vacuum; and w_0 is the radius of the mode in the waist.

We will seek the solution in the form

$$U = A\exp\left(-\frac{ink}{2q(z)}r^2\right)\exp(-iF(z)),$$

after which equation (2) takes the form

$$-\frac{2ink}{q} - r^2\frac{n^2k^2}{q^2} + r^2\frac{n^2k^2}{q^2}q' - 2n^2kF' + \frac{4\pi}{P_{cr,G}}|U|^2 = 0. \tag{A4}$$

We shall consider the problem at powers less than the critical value $P_{cr,G}$. Then we can use the method of successive approximations. Letting $P_{cr,G}$ approach infinity and separating the terms at r^0 and r^2, we obtain the linear approximation

$$q_{lin}(z) = z - z_0 + nq_0, \tag{A5.1}$$

$$F_{lin}(z) = -i\ln\left(\frac{q_{lin}}{nq_0}\right) + F_0. \tag{A5.2}$$

Now we substitute a linear solution for $|U|^2$ and replace it with a parabola with respect to r with equal area and height

$$|U|^2 \approx |U_{lin}|^2 \Rightarrow A^2\left(1 - \frac{nk\,\mathrm{Im}\,q_{lin}}{2|q_{lin}|^2}r^2\right)\frac{|nq_0|^2}{|q_{lin}|^2}. \tag{A6}$$

In this case, equation (A4) takes the form:

$$-\frac{2ink}{q} - r^2\frac{n^2k^2}{q^2} + r^2\frac{n^2k^2}{q^2}q' - 2n^2kF' + \\ + \frac{4\pi}{P_{cr,G}}A^2\left(1 - \frac{nk\,\mathrm{Im}\,q_{lin}}{2|q_{lin}|^2}r^2\right)\frac{|nq_0|^2}{|q_{lin}|^2} = 0. \tag{A7}$$

Here we can also separate the terms for r^0 and r^2, i.e., the beam remains Gaussian, but with a nonlinear correction to q:

$$-\frac{k}{q^2} + \frac{k}{q^2}q' - \frac{2\pi}{P_{cr,G}}A^2\frac{n\,\mathrm{Im}\,q_{lin}|q_0|^2}{|q_{lin}|^4} = 0, \tag{A8}$$

$$-\frac{2ink}{q} - 2n^2kF' + \frac{4\pi}{P_{cr,G}}A^2\frac{|nq_0|^2}{|q_{lin}|^2} = 0. \tag{A9}$$

We leave only the first equation, since the second one contains only the phase and normalisation to the power. We express A^2 through power P:

$$P = \int_0^\infty |U_0|^2 2\pi r\,dr = \pi A^2\frac{|q_0|^2}{kz_{R,0}}, \tag{A10}$$

$$A^2 = \frac{Pkz_{R,0}}{\pi|q_0|^2}. \tag{A11}$$

Then equation (A8) takes the form

$$q' = 1 + \frac{2P}{P_{cr,G}}\frac{n^2z_{R,0}^2}{|q_{lin}|^4}q^2 \approx 1 + \frac{2P}{P_{cr,G}}\frac{n^2z_{R,0}^2}{(q_{lin}^*)^2}. \tag{A12}$$

Hence we obtain

$$q = q_{lin} - \frac{2P}{P_{cr,G}}n^2z_{R,0}^2\left(\frac{1}{q_{lin}^*} - \frac{1}{nq_0^*}\right) \\ = q_{lin} + \frac{2P}{P_{cr,G}}\frac{nz_{R,0}^2}{|q_0|^2}\frac{(z-z_0)q_0}{q_{lin}^*}, \tag{A13}$$

so that after a layer of thickness h from the outside of the boundary

$$q = \frac{h}{n} + q_0 + 2\frac{P}{P_{cr,G}}\frac{z_{R,0}^2}{|q_0|^2}\frac{(h/n)q_0}{(h/n + q_0^*)}. \tag{A14}$$

We note immediately that the nonlinear correction will be real if $z_0 = -h/(2n)$, i.e., when in the linear case the position of the waist is exactly in the middle of the plate.

In the case of a real additive

$$q = (z - z_0 - h) + \frac{h}{n} - 2\frac{P}{P_{cr,G}}\frac{z_{R,0}^2}{|q_0|^2}\frac{h}{n} + iz_{R,0} \tag{A15}$$

and only the position of the waist of the Gaussian beam changes (it will move forward, as shown in Fig. 1).

Detuning inside the glass is

$$\Delta(P, z_{R,0}) = 2\frac{P}{P_{cr,G}}h\frac{z_{R,0}^2}{h^2/2n + z_{R,0}^2}, \tag{A16}$$

and after the glass the detuning is equal to Δ/n.

Let the beam pass through the nonlinear plate, and then be focused it into fibre by two optical lenses (see Fig. 1), and let us assume that the waist at a low power is in the middle of the plate. A lens with a focal length f converts the Gaussian beam parameter q as follows [14]:

$$\frac{1}{q_1 + a} - \frac{1}{f} = \frac{1}{q_2 - b}. \tag{A17}$$

If q_1 has the form

$$q_1 = \frac{h}{n} - \frac{\Delta(P, z_{R,0})}{n} + iz_{R,0}, \tag{A18}$$

then the real part q_1 can be interpreted as a change in the value of a:

$$\frac{1}{iz_{R,0} + a + (h/n) - (\Delta(P, z_{R,0})/n)} - \frac{1}{f} = \frac{1}{q^2 - b}. \tag{A19}$$

Let

$$\gamma = a + \frac{h}{n} - \frac{\Delta(P, z_{R,0})}{n}. \tag{A20}$$

Then the beam parameters before entering the fibre have the following form. The imaginary part is

$$\operatorname{Im} q = Z_{\mathrm{R,new}}(\gamma, b, z_{\mathrm{R},0}) = \frac{z_{\mathrm{R},0} f_1^2 f_2^2}{[\gamma(\gamma - f_2^2) - f_1(\gamma + b - f_1)]^2 + z_{\mathrm{R},0}^2(-b + f_1 + f_2)^2}, \quad \text{(A21)}$$

and the real part is

$$\operatorname{Re} q = d_{\mathrm{new}}(\gamma, b, z_{\mathrm{R},0}) = \frac{f_2[-b(\gamma^2 + z_{\mathrm{R},0}^2)(b - f_2) - f_1^2((\gamma + b)^2 + z_{\mathrm{R},0}^2 - (\gamma + b)f_2)]}{[\gamma(\gamma - f_2^2) - f_1(\gamma + b - f_1)]^2 + z_{\mathrm{R},0}^2(-b + f_1 + f_2)^2} + \frac{f_2 f_1[2b(\gamma^2 + 2\gamma b + z_{\mathrm{R},0}^2) - (\gamma^2 + 2\gamma b + z_{\mathrm{R},0}^2)f_2]}{[\gamma(\gamma - f_2^2) - f_1(\gamma + b - f_1)]^2 + z_{\mathrm{R},0}^2(-b + f_1 + f_2)^2}. \quad \text{(A22)}$$

We calculate the overlap integral of the field of the coupled light U with the field of the mode emerging from the optical fibre, which is approximated by the Gaussian profile:

$$U_{\mathrm{f}} = B \exp\left(-\frac{kr^2}{2z_{\mathrm{R,i}}}\right), \quad \text{(A23)}$$

where $z_{\mathrm{R,i}}$ is the parameter of the beam emerging from the optical fibre. Then the overlap integral $I = \langle U|U_{\mathrm{f}}\rangle^2/[\langle U|U\rangle\langle U_{\mathrm{f}}|U_{\mathrm{f}}\rangle]$ takes the form

$$I(\gamma, b, z_{\mathrm{R},0}, x) = \frac{4 z_{\mathrm{R,i}} Z_{\mathrm{R,new}}(\gamma, b, z_{\mathrm{R},0})}{(x + d_{\mathrm{new}}(\gamma, b, z_{\mathrm{R},0}))^2 + (z_{\mathrm{R,i}} + Z_{\mathrm{R,new}}(\gamma, b, z_{\mathrm{R},0}))^2}, \quad \text{(A24)}$$

where x is the detuning of the optical fibre from the position corresponding to the maximum of the output coupling ratio.

The value of $z_{\mathrm{R},0}$ can be found from the output coupling ratio T_{meas} measured at a low power, by solving the equation

$$I\left(a + \frac{h}{n}, b, z_{\mathrm{R},0}, 0\right) = T_{\mathrm{meas}}. \quad \text{(A25)}$$

As a result, in the experiment we will have an output coupling ratio directly proportional to the overlap integral

$$I\left(a + \frac{h}{n} - \frac{\Delta(P, z_{\mathrm{R},0})}{n}, b, z_{\mathrm{R},0}, x\right). \quad \text{(A26)}$$

References

1. Osellame R., Cerullo G., Ramponi R. *Femtosecond Laser Micromachining: Photonic and Microfluidic Devices in Transparent Materials* (Springer Science & Business Media, 2012).
2. Kryukov P.G. *Quantum Electron.*, **31**, 95 (2001) [*Kvantovaya Elektron.*, **31**, 95 (2001)].
3. Keller U. et al. *IEEE J. Sel. Top. Quantum Electron.*, **2**, 435 (1996).
4. Zhang M. et al. *Opt. Lett.*, **36**, 3984 (2011).
5. Sotor J. et al. *Opt. Express*, **22**, 5536 (2014).
6. Fermann M.E. et al. *Opt. Lett.*, **18**, 894 (1993).
7. Morgner U. et al. *Opt. Lett.*, **24**, 411 (1999).
8. Wang L. et al. *Opt. Commun.*, **383**, 292 (2016).
9. Wang L. et al. *Opt. Commun.*, **383**, 386 (2017).
10. Smektala F. et al. *J. Non-Crystal. Solids*, **239**, 139 (1998).
11. Turitsyn S.K. et al. *Opt. Express*, **15**, 14750 (2007).
12. Kalosha V.P., Liang Chen, Xiaoyi Bao. *Proc. SPIE*, **7099**, 70990S (2008).
13. Talanov V.I. *JETP Lett.*, **11** (6), 199 (1970) [*Pis'ma Zh. Eksp. Teor. Fiz.*, **11** (6), 303 (1970)]; Vlasov S.N., Petrishchev V.A., Talanov V.I. *Radiophys. Quantum Electron.*, **14** (9), 1062 (1971) [*Izv. Vyssh. Uchebn. Zaved., Ser. Radiofiz.*, **14** (9), 1353 (1971)].
14. Yariv A. *Introduction to Optical Electronics* (Oxford: Oxford University Press, 1991; Moscow: Vysshaya shkola, 1983).